

- 2, Vol. II A, 1966 (unpublished).
- ⁶P. Chiotti, J. T. Mason, and K. J. Gill, *Trans. AIME* **221**, 573 (1961).
- ⁷J. P. Jan, Division of Pure Physics, National Research Council, Ottawa, Canada (private communication).
- ⁸B. N. Brockhouse, in *Inelastic Scattering of Neutrons in Solids and Liquids* (International Atomic Energy Agency, Vienna, 1961), p. 113.
- ⁹T. O. Brun and S. K. Sinha (unpublished).
- ¹⁰A. J. E. Foreman and W. M. Lomer, *Proc. Phys. Soc. (London)* **70**, 1143 (1957).
- ¹¹G. L. Squires, in *Inelastic Scattering of Neutrons in Solids and Liquids* (International Atomic Energy Agency, Vienna, 1963), Vol. II, p. 125.
- ¹²T. S. Preveder, U. S. Atomic Energy Commission Report No. IS-2185, 1969 (unpublished).
- ¹³J. K. Boyter and H. L. McMurry, U. S. Atomic Energy Commission Report No. IN-1148, 1967 (unpublished).
- ¹⁴J. L. Warren, *Rev. Mod. Phys.* **40**, 38 (1968).
- ¹⁵J. Daubert, *Phys. Letters* **32A**, 437 (1970).
- ¹⁶R. S. Leigh, B. Szigeti, and V. K. Tewary, *Proc. Roy. Soc. (London)* **A320**, 505 (1971).
- ¹⁷See, e.g., O. Kubaschewski, in *The Physical Chemistry of Metallic Solutions and Intermetallic Compounds* (Her Majesty's Stationery Office, London, 1959), Paper 3C.
- ¹⁸L. J. Raubenheimer and G. Gilat, U. S. Atomic Energy Commission Report No. ORNL-TM-1425, 1966 (unpublished).
- ¹⁹G. Gilat and L. J. Raubenheimer, *Phys. Rev.* **144**, 390 (1966).
- ²⁰L. Van Hove, *Phys. Rev.* **89**, 1189 (1953).

Localized d States for Pseudopotential Calculations: Application to the Alkaline-Earth Metals*

John A. Moriarty

University of California, Los Alamos Scientific Laboratory, Los Alamos, New Mexico 87544

(Received 24 July 1972)

A procedure for constructing very localized d basis states for generalized pseudopotential calculations is suggested and applied to the alkaline-earth metals calcium, strontium, and barium. Unlike the d states of the free ion or atom, these localized d states do not significantly overlap their neighbors in the metal. They also appear to lead to more accurate estimates of the s - d hybridization. Form factors and energy-wave-number characteristics are calculated and used to study the effects of hybridization on representative physical properties of the alkaline earths. In general, hybridization is found to make important contributions to the liquid-metal resistivity and the low-temperature-phase stability, but not to the binding energy nor to the phonon frequencies. A preliminary calculation also suggests that the fcc-bcc phase transitions in calcium and strontium can be understood in terms of the generalized pseudopotential theory.

I. INTRODUCTION

The generalization of pseudopotential theory to the d -band metals¹⁻³ relies on a power-series expansion of the electron density and the total energy in each of two small quantities. The first of these quantities is a pseudopotential w_0 , which is exactly analogous to the pseudopotential entering the simple-metal theory. The second is a hybridization potential Δ , which embodies the fact that ionic or atomic d states are not good eigenstates of the crystal Hamiltonian H . Formally, if one defines a set of localized d states $|\varphi_d\rangle$ by the Schrödinger equation

$$H^t |\varphi_d\rangle = E_d^t |\varphi_d\rangle, \quad (1)$$

then the hybridization potential Δ can be expressed in the form

$$\Delta = \delta V - \langle \varphi_d | \delta V | \varphi_d \rangle, \quad (2)$$

where

$$\delta V = H^t - H. \quad (3)$$

In principle, one is free to choose H^t at will, so long as the $|\varphi_d\rangle$ remain orthogonal to the core states of the metal $|\varphi_c\rangle$ (which are assumed to be eigenfunctions of H). In a given calculation, if one were to keep terms of all orders in w_0 and Δ , then the result would be independent of the choice of H^t . Of course, one always wishes to terminate these expansions at a finite order (e.g., first order in Δ^2 and w_0 for the electron density and second order in these quantities for the total energy), and thus the result one obtains will generally reflect the choice of H^t .

In practice, the most obvious procedure is to take H^t as the Hamiltonian of the free ion or atom, as we did recently with the noble metals.^{4,5} Then δV is, for example, the difference in potential seen by an electron in a free ion and an electron in the vicinity of an ion site in the metal, and the hybridization potential Δ can be expected to be small, at least inside the core region of the ion. Free-ion d states, however, may extend well out-

side the core, and hence this δV may not minimize the strength of the hybridization potential, as would be expected for the optimum choice of H^i . Moreover, the tails of the ionic d states centered on neighboring ion sites in the metal overlap, and this overlap is not negligible. This not only complicates the theory but makes its practical application uncertain because the evaluation of overlap matrix elements like $\langle \varphi_a | \Delta | \varphi_a \rangle$ is extremely difficult at best.

The above problems become more serious as one moves from the noble metals to the left in the Periodic Table, because the effective spatial extent of the ionic d state is increased. In the alkaline-earth metals, in fact, the d states in the free ion are unoccupied and extend far beyond the radius of the unit cell of the metal. In this paper we suggest a simple calculational procedure for constructing a more useful set of d states for pseudopotential calculations on such metals. In this procedure, we localize $\langle \vec{r} | \varphi_d \rangle$ within the unit cell of the metal by adding to the free-ion Hamiltonian a suitable attractive potential. The d states on a given ion site are easily localized to the degree that overlap with their neighbors becomes negligible. At the same time, the effective strength of the hybridization is decreased and becomes relatively insensitive to further changes in H^i .

Highly localized d basis states have been used previously in modified-orthogonalization-plane-wave (OPW) methods⁸ to speed the convergence of the d -like states in the calculation of the band structure. Although the point of view in such approaches is quite similar to ours, we are not concerned here with a direct calculation of the energy eigenvalue spectrum itself. For this reason, the details of our method are somewhat different than those of the modified-OPW methods.

In Sec. II we consider the construction of localized d states for the alkaline-earth metals calcium, strontium, and barium. We then proceed to demonstrate the explicit advantages of these basis states in generalized pseudopotential calculations. The alkaline earths are prototypes of metals with empty d bands lying above the Fermi level and are especially interesting because they have historically been treated as simple metals in pseudopotential calculations.^{7,8} After reviewing the relevant formalism in Sec. III, we shall study the relationship of the hybridization to $|\varphi_d\rangle$ in Sec. IV and the effect of the hybridization on the properties of the alkaline-earth metals in Sec. V.

II. LOCALIZATION OF $\langle \vec{r} | \varphi_d \rangle$

We begin by considering free-ion-like calculations with a Hamiltonian

$$H^i = T + v^{ion}, \quad (4)$$

where T is the kinetic-energy operator and v^{ion} is a spherically symmetric potential of the form

$$v^{ion}(r) = v^{Coul}(r) + v^{ex}(r) + v^{loc}(r). \quad (5)$$

The quantity $v^{Coul}(r)$ represents the Coulomb potential arising from the nucleus and the electron density of filled core states. The net charge on the ion is $+Ze$, where Z is the appropriate metallic valence. (For the alkaline-earth metals, $Z=2$.)

For $v^{ex}(r)$ we use a free-electron exchange potential of the form⁹

$$v^{ex}(r) = -4 \left\{ \left[\frac{3}{8\pi} \left(\sum_c \langle \vec{r} | \varphi_c \rangle \langle \varphi_c | \vec{r} \rangle + \frac{Z}{\Omega_0} \right) \right]^{1/3} - \left(\frac{3}{8\pi} \frac{Z}{\Omega_0} \right)^{1/3} \right\}, \quad (6)$$

where Ω_0 is the appropriate atomic volume of the metal and the sum runs over the filled core states. This is a suitable form for the valence-core exchange potential in the metal (although this form is slightly different from the one we used previously⁵). The first term on the right-hand side of Eq. (6) gives (to zero order) the total exchange potential near an ion in the metal, while the second term subtracts the self-exchange of the valence electrons, which is included separately.

The last term on the right-hand side of Eq. (5) represents the arbitrary attractive potential which we wish to use to better localize the unoccupied d state about the origin. In our calculations, we have considered only two closely related forms for $v^{loc}(r)$. The first of these is a square-well potential

$$v^{loc}(r) = \begin{cases} -\alpha_{sw} Z / R_{sw}, & r < R_{sw} \\ 0, & r > R_{sw} \end{cases} \quad (7)$$

where α_{sw} and R_{sw} are constants. (The use of this potential will hereafter be referred to as method 1.) The general idea here is to choose R_{sw} approximately equal to the Wigner-Seitz radius R_{ws} in the metal. (The actual values of R_{sw} and R_{ws} used in our calculations are given in Table I.) Then the core wave functions will be modified only slightly by v^{loc} , while, for sufficiently large α_{sw} , the d wave function will be well localized within the Wigner-Seitz cell. In practice, this method

TABLE I. Parameters for the alkaline-earth metals used in the present calculations, in a.u.

Metal	Z	Ω_0	E_F	k_F	R_{ws}	R_{sw}
Ca	2	290.0	0.3468	0.5889	4.106	3.725
Sr	2	373.6	0.2929	0.5412	4.468	4.019
Ba	2	424.3	0.2690	0.5137	4.662	4.124

is not entirely satisfactory because the perturbation of the outer core states (e.g., the $3s$ and $3p$ states in calcium) turns out not to be negligible in general. This will be demonstrated quantitatively in Sec. IV. A preferable approach (hereafter referred to as method 2) is to let v^{10c} operate only on the unoccupied d state. This can be accomplished mathematically by multiplying v^{10c} by a projection operator

$$P_2 = \sum_{m=-2}^{+2} |Y_{2m}\rangle\langle Y_{2m}|, \quad (8)$$

where $|Y_{2m}\rangle$ is the usual $l=2$ spherical harmonic. The operator P_2 has the effect of operating v^{10c} only on states of d symmetry. The core states of d symmetry, i.e., the $3d$ state in strontium and the $3d$ and $4d$ states in barium, are sufficiently localized so that v^{10c} has no important effect on them and in practice it is unnecessary to include v^{10c} in calculating these states.

For the Hamiltonian given by Eq. (4), the core and d wave functions, $\langle \vec{r} | \varphi_c \rangle$ and $\langle \vec{r} | \varphi_d \rangle$, have the familiar form

$$[P_{nl}(r)/r]Y_{lm}(\vec{r}),$$

where n , l , and m are the usual quantum numbers and $P_{nl}(r)$ satisfies the radial Schrödinger equation

$$-\frac{d^2 P_{nl}(r)}{dr^2} + \left(v^{10a}(r) + \frac{l(l+1)}{r^2} - E_{nl}^i \right) P_{nl}(r) = 0. \quad (9)$$

In all of our calculations we have used a suitably modified form of the Herman-Skillman computer program¹⁰ to solve Eq. (9) self-consistently for each v^{10a} of interest. Specifically, we have calculated the appropriate P_{nl} and E_{nl}^i for calcium, strontium, and barium with both methods 1 and 2 for various values of α_{sw} . Figure 1 illustrates how the $3d$ radial wave function (P_{3d}) in calcium is localized as a function of α_{sw} through use of method 2. Note that $P_{3d}(r)$ is changed rather significantly near R_{ws} and beyond by a small v^{10c} , but that the wave function becomes relatively insensitive to the depth of the square well for $\alpha_{sw} > 5$. The same qualitative picture emerges in method 1, although the localization is slightly less rapid as a function of α_{sw} . The localization of $\langle \vec{r} | \varphi_d \rangle$ accomplished with $\alpha_{sw} \geq 5$ is sufficient to make d -state overlap negligible, as we shall show in Sec. V.

III. PSEUDOPOTENTIAL FORMALISM

The wave functions and term values generated from the solution of Eq. (9) can be used directly in the generalized pseudopotential formalism to make calculations on the alkaline-earth metals. Before discussing such calculations, we shall briefly review the basic theory¹⁻⁵ as it applies to

metals with empty d bands above the Fermi level.

The two principal theoretical quantities of interest are the form factor and the total energy. The form factor is given by the matrix element

$$\langle \vec{k} + \vec{q} | w | \vec{k} \rangle = \langle \vec{k} + \vec{q} | w_0 | \vec{k} \rangle - \sum_d \frac{\langle \vec{k} + \vec{q} | \Delta | \varphi_d \rangle \langle \varphi_d | \Delta | \vec{k} \rangle}{E_d - k^2} \quad (10)$$

evaluated on the free-electron Fermi sphere (i.e., $|\vec{k} + \vec{q}| = |\vec{k}| = k_F$), where $\langle \vec{r} | \vec{k} \rangle = \Omega_0^{-1/2} e^{i\vec{k} \cdot \vec{r}}$ and

$$\begin{aligned} \langle \vec{k} + \vec{q} | w_0 | \vec{k} \rangle &= \langle \vec{k} + \vec{q} | v | \vec{k} \rangle \\ &+ \sum_{\alpha=c,d} (k^2 - E_\alpha) \langle \vec{k} + \vec{q} | \varphi_\alpha \rangle \langle \varphi_\alpha | \vec{k} \rangle \\ &+ \sum_d \langle \vec{k} + \vec{q} | \Delta | \varphi_d \rangle \langle \varphi_d | \vec{k} \rangle + c.c. \end{aligned} \quad (11)$$

In Eq. (11) we have used the simplified Austin form¹¹ of the pseudopotential rather than the Cohen-Heine form¹² used previously.^{4,5} The Fourier transform of the self-consistent potential v may be written

$$\begin{aligned} v_q &= \langle \vec{k} + \vec{q} | v | \vec{k} \rangle \\ &= \frac{8\pi}{q^2 \epsilon^*(q)} \left(-\frac{Z}{\Omega_0} + (n_q^{\text{core}} - n_0^{\text{core}}) + \frac{q^2}{8\pi} v_q^{\text{ex}} \right. \\ &\quad \left. + [1 - G(q)](n_q^{\text{oh}} + n_q^R) \right), \end{aligned} \quad (12)$$

where n_q^{core} , v_q^{ex} , and n_q^{oh} are, respectively, the Fourier transforms of the core-electron density, the valence-core exchange potential [Eq. (6)], and the orthogonalization hole density,

$$\begin{aligned} n^{\text{oh}}(r) &= -[2\Omega_0/(2\pi)^3] \int_{k < k_F} d^3k [\langle \vec{r} | P | \vec{k} \rangle \langle \vec{k} | \vec{r} \rangle \\ &\quad + c.c.] - \langle \vec{r} | P | \vec{k} \rangle \langle \vec{k} | P | \vec{r} \rangle, \end{aligned} \quad (13)$$

where $P = \sum_{\alpha=c,d} |\varphi_\alpha\rangle\langle\varphi_\alpha|$. (Note that the orthogonalization hole density includes a sum over d states as well as core states.) The quantity n_q^R is given by

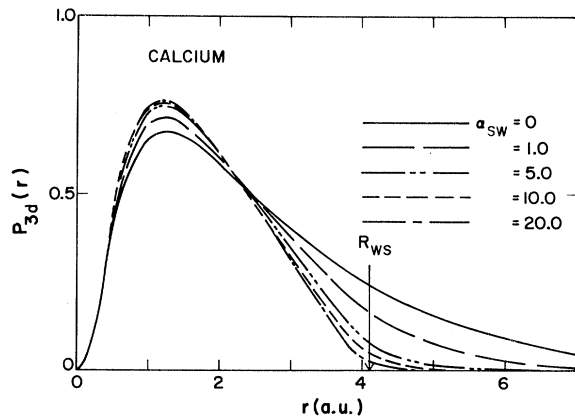


FIG. 1. $3d$ radial wave function of calcium for five different values of the square-well depth.

$$n_a^R = \frac{4}{(2\pi)^3} \int_{k < k_F} d^3k \left[\frac{\langle \vec{k} + \vec{q} | w | \vec{k} \rangle - v_a}{k^2 - |\vec{k} + \vec{q}|^2} - \sum_d \left(\frac{\langle \vec{k} | \varphi_d \rangle \langle \varphi_d | e^{-i\vec{q} \cdot \vec{r}} | \varphi_d \rangle \langle \varphi_d | \Delta | \vec{k} \rangle}{E_d - k^2} - \frac{\langle \vec{k} + \vec{q} | \varphi_d \rangle \langle \varphi_d | \Delta | \vec{k} \rangle}{E_d - k^2} - \frac{\langle \vec{k} | \Delta | \varphi_d \rangle \langle \varphi_d | e^{-i\vec{q} \cdot \vec{r}} | \varphi_d \rangle \langle \varphi_d | \Delta | \vec{k} \rangle}{2(E_d - k^2)^2} \right) \right] \quad (14)$$

The quantities $G(q)$ and $\epsilon^*(q)$ are the usual exchange-correlation function for the electron gas and the dielectric function as modified by $G(q)$, respectively. In all of our calculations, we have used the interpolation formula for $G(q)$ suggested by Singwi *et al.*,¹³ as we did recently⁵ with the noble metals.

The zero of energy in terms like $(k^2 - E_c)$ is chosen at the bottom of the conduction band, so that $\langle 0 | w | 0 \rangle = 0$, where $|0\rangle$ equals $|\vec{k}\rangle$ at $\vec{k} = 0$. Since $\langle 0 | \Delta | \varphi_d \rangle = \langle 0 | \varphi_d \rangle = 0$, Eqs. (10) and (11) lead one to the following identity for the expectation value of H between core states:

$$E_c = \langle \varphi_c | H | \varphi_c \rangle \\ \equiv - \left((v_0 - E_c) + \frac{\sum_{c'} (v_0 - E_{c'}) \langle 0 | \varphi_{c'} \rangle \langle \varphi_{c'} | 0 \rangle}{1 - \sum_{c'} \langle 0 | \varphi_{c'} \rangle \langle \varphi_{c'} | 0 \rangle} \right), \quad (15)$$

where v_0 equals v_a at $q = 0$. In Eq. (11) one needs E_c and hence $v_0 - E_c$ only to lowest order. The latter quantity is easily evaluated to zero order:

$$E_{te} = \frac{3}{5} Z k_F^2 + E_{xc} + Z^* \left(-\frac{4\pi}{3\Omega_0} \sum_c \langle \varphi_c | r^2 | \varphi_c \rangle + v_0^{ex} \right) - \frac{1}{2} \int d^3r v^{oh}(r) n^{oh}(r) \\ + \frac{2\Omega_0}{(2\pi)^3} \int_{k < k_F} d^3k \left[\left(\sum_{\alpha=c,d} T_\alpha(\vec{k}) \langle \vec{k} | \varphi_\alpha \rangle \langle \varphi_\alpha | \vec{k} \rangle + \sum_d \langle \vec{k} | \Delta | \varphi_d \rangle \langle \varphi_d | \vec{k} \rangle + \text{c.c.} \right) (1 + \langle \vec{k} | P | \vec{k} \rangle) \right. \\ \left. - \sum_d \frac{\langle \vec{k} | \Delta | \varphi_d \rangle \langle \varphi_d | \Delta | \vec{k} \rangle}{E_d - k^2} \left(1 + \langle \vec{k} | P | \vec{k} \rangle + \frac{\langle \vec{k} | w_0 | \vec{k} \rangle}{E_d - k^2} - \sum_{d'} \frac{\langle \vec{k} | \Delta | \varphi_{d'} \rangle \langle \varphi_{d'} | \Delta | \vec{k} \rangle}{(E_d - k^2)^2} \right) \right], \quad (19)$$

where Z^* is the usual effective valence,

$$Z^* = Z - (1/\Omega_0) \int d^3r n^{oh}(r), \quad (20)$$

and

$$T_\alpha(\vec{k}) = k^2 + \frac{\langle \varphi_\alpha | (Z^* - Z) r^2 / R_{ws}^3 - v^{oh}(r) | \varphi_\alpha \rangle}{1 + \langle \vec{k} | P | \vec{k} \rangle} - E_\alpha^i + \langle \varphi_\alpha | \delta V | \varphi_\alpha \rangle. \quad (21)$$

The quantity E_{xc} represents various exchange-correlation terms⁵ for the valence electrons, and in all calculations we have approximated E_{xc} by the standard formula¹⁴ for a uniform electron gas of density Z/Ω_0 .

The remaining three terms in E_{total} depend explicitly on the positions of the ions. The band-structure energy E_{bs} can be written

$$v_0 - E_c = -\frac{18}{5} \frac{Z}{R_{ws}} - \frac{4\pi}{3\Omega_0} \sum_{c'} \langle \varphi_{c'} | r^2 | \varphi_{c'} \rangle + v_0^{ex} - E_c^i + \langle \varphi_c | \delta V | \varphi_c \rangle, \quad (16)$$

where E_c^i is the appropriate ionic term value [i. e., E_{ni}^i in Eq. (9)] and v_0^{ex} equals v_a^{ex} at $q = 0$. The calculation of δV is discussed below. Equations (15) and (16) also hold for the position of the d resonance,

$$E_d = \langle \varphi_d | H | \varphi_d \rangle, \quad (17)$$

with E_c , E_c^i , and $|\varphi_c\rangle$ replaced by E_d , E_d^i , and $|\varphi_d\rangle$, respectively.

The total energy (per ion) E_{total} can be written as a sum of four contributions:

$$E_{total} = E_{te} + E_{bs} + E_{es} + E_{o1}. \quad (18)$$

The formula for the free-electron energy E_{te} is complicated but this quantity is, nevertheless, independent of the ion configuration to second order:

$$E_{bs} = \sum_i' |S(\vec{q})|^2 F(q), \quad (22)$$

where $S(\vec{q})$ is the usual structure factor $N^{-1} \sum_i e^{-i\vec{q} \cdot \vec{r}_i}$ (with \vec{r}_i denoting the position of the i th ion) and where the prime means that the $\vec{q} = 0$ term is to be omitted from the sum. The energy-wave-number characteristic $F(q)$ takes the familiar simple-metal form

$$F(q) = \frac{2\Omega_0}{(2\pi)^3} \int_{k < k_F} d^3k \frac{|\langle \vec{k} + \vec{q} | w | \vec{k} \rangle|^2}{k^2 - |\vec{k} + \vec{q}|^2} - \frac{4\pi\Omega_0}{q^2} \{ [1 - G(q)] |n_a^{sc}|^2 + G(q) |n_a^{oh}|^2 \}, \quad (23)$$

where n_a^{sc} is the Fourier transform of the screening electron density and is given by Eq. (14) minus the single term involving v_a . The quantity E_{es} is the usual electrostatic or Ewald energy per ion of

N point ions of charge Z^*e immersed in a uniform compensating background. Last, E_{o1} is the overlap energy which accompanies the overlapping basis states $|\varphi_d\rangle$. This energy can be written

$$E_{o1} = \frac{1}{2N} \sum'_{i,j} v_{o1}(\vec{r}_i - \vec{r}_j), \quad (24)$$

where the sums of i and j are over all ion positions \vec{r}_i and \vec{r}_j ($\vec{r}_i = \vec{r}_j$ excluded) and

$$v_{o1}(\vec{r}_i - \vec{r}_j) = \frac{2\Omega_0}{(2\pi)^3} \int_{k < k_F} d^3k \left\{ \sum_{a,a'} \left[\langle \varphi_a | \varphi_{a'} \rangle \left((E_d - k^2) \langle \varphi_{a'} | \vec{k} \rangle \langle \vec{k} | \varphi_a \rangle - \langle \varphi_{a'} | \vec{k} \rangle \langle \vec{k} | \Delta | \varphi_a \rangle + \text{c. c.} \right) + \frac{\langle \varphi_{a'} | \Delta | \vec{k} \rangle \langle \vec{k} | \Delta | \varphi_a \rangle}{E_d - k^2} \right. \right. \\ \left. \left. + \langle \varphi_a | \Delta | \varphi_{a'} \rangle \left(\langle \varphi_{a'} | \vec{k} \rangle \langle \vec{k} | \varphi_a \rangle - \frac{\langle \varphi_{a'} | \vec{k} \rangle \langle \vec{k} | \Delta | \varphi_a \rangle + \text{c. c.}}{E_d - k^2} - \frac{\langle \varphi_{a'} | \Delta | \vec{k} \rangle \langle \vec{k} | \Delta | \varphi_a \rangle}{(E_d - k^2)^2} \right) + \text{c. c.} \right] \right\}. \quad (25)$$

In Eq. (25), $\langle \vec{r} | \varphi_d \rangle$ is centered on ion site i while $\langle \vec{r} | \varphi_{a'} \rangle$ is centered on ion site j .

IV. HYBRIDIZATION AND $|\varphi_d\rangle$

The localization of $\langle \vec{r} | \varphi_d \rangle$ by the methods discussed in Sec. II can make the matrix elements $\langle \varphi_a | \varphi_{a'} \rangle$ and $\langle \varphi_a | \Delta | \varphi_{a'} \rangle$, and hence the overlap energy, vanishingly small. This localization, of course, will also affect the hybridization terms in $\langle \vec{k} + \vec{q} | w | \vec{k} \rangle$, E_{te} , and $F(q)$ through the position of the resonance E_d and the hybridization matrix element $\langle \vec{k} | \Delta | \varphi_d \rangle$. We now consider how v^{loc} will affect these latter two quantities.

To evaluate the quantities E_d and $\langle \vec{k} | \Delta | \varphi_d \rangle$ one needs only to compute the potential δV to zero order. In our calculations we have taken

$$\delta V(r) = v^{loc}(r) + Zr^2/R_{WS}^3 + \text{const.} \quad (26)$$

The second term on the right-hand side of Eq. (26) is (the negative of) the Coulomb potential arising from a uniform electron gas of density Z/Ω_0 . The constant term in Eq. (26) includes the

exchange-correlation potential associated with the uniform electron gas and, as an approximation, the potential due to the neighboring ions in the metal. In Eqs. (16) and (21) it is appropriate to set this constant equal to zero. The constant also makes no contribution to the hybridization potential Δ , as is obvious from Eq. (2).

From Eqs. (15)–(17), it is clear that with localization method 2, one may write

$$E_d = E_d^i - \langle \varphi_d | \delta V | \varphi_d \rangle + C, \quad (27)$$

where C is a constant independent of v^{loc} . In Fig. 2 we have plotted the change in E_d as a function of α_{sw} for calcium, strontium, and barium. In each case note that E_d moves upward in energy and approaches a limiting value as $\alpha_{sw} \rightarrow \infty$. Figure 2 also shows the corresponding results we obtained with method 1. In method 1, C is no longer a constant but increases as a function of α_{sw} . The error introduced into E_d by method 1 can clearly be a significant fraction of total change in E_d due to v^{loc} . For this reason method 2 is preferred. The remainder of the calculations described in Secs. IV and V of this paper were performed with this method.

Although there have been a number of band-structure calculations done on the alkaline-earth metals, especially calcium, the position of the d band does not seem to be very well established in any of these metals. Nevertheless, it is interesting to compare our values of E_d with the information available in the literature about the mean position of the d band for each of the alkaline earths. Table II lists the values of both E_d and $E_d - E_F$ we have obtained through use of Eq. (26) together with estimates of these quantities we have made from band-structure calculations. Note that for each metal all five of our values of E_d lie between the extremes of the band-structure results. For $\alpha_{sw} \geq 5$ the same is true of our calculated $E_d - E_F$.

Also listed in Table II are the corresponding values we have calculated for the half-width of the d resonance,

$$\frac{1}{2} W_d = \Omega_0 k_d \Delta^2(k_d), \quad (28)$$

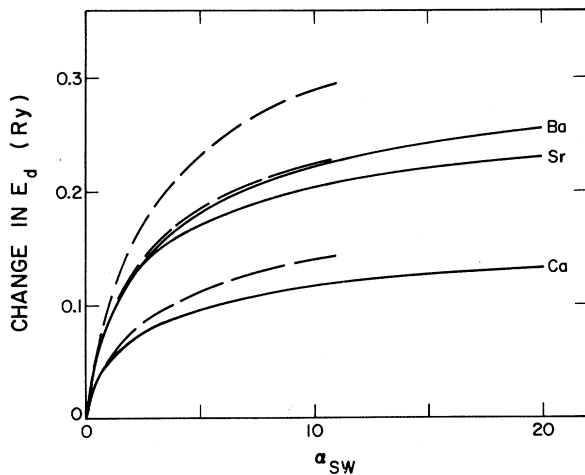


FIG. 2. Change in the position of the d resonance as a function of square-well depth for calcium, strontium, and barium. The dashed lines refer to method 1 and the solid lines to method 2, as explained in the text.

TABLE II. The position and half-width of the d resonance for the alkaline-earth metals, in Ry.

Metal	Estimates from band calculations	Present work with $\alpha_{sw} =$				
		0.0	1.0	5.0	10.0	20.0
$E_d(E_d - E_F)$						
Ca	>0.90 (>0.57) ^a 0.47 (0.19) ^b 0.56, 0.60 ^c 0.65 (0.34) ^d	0.520 (0.173)	0.569 (0.222)	0.617 (0.270)	0.636 (0.290)	0.653 (0.306)
Sr	>0.82 (>0.53) ^a 0.45 (0.20) ^b 0.56 ^c	0.452 (0.159)	0.540 (0.247)	0.623 (0.330)	0.655 (0.362)	0.683 (0.390)
Ba	>0.76 (>0.49) ^a 0.34 (0.18) ^b 0.63 ^c	0.350 (0.081)	0.436 (0.167)	0.531 (0.262)	0.571 (0.302)	0.606 (0.336)
$\frac{1}{2}W_d$						
Ca	...	0.086	0.106	0.125	0.135	0.143
Sr	...	0.088	0.141	0.200	0.225	0.249
Ba	...	0.143	0.168	0.236	0.271	0.306

^aB. Vasvári, A. O. E. Animalu, and V. Heine, Phys. Rev. **154**, 535 (1967); B. Vasvári, Rev. Mod. Phys. **40**, 776 (1968). The values of E_d are the $(\Gamma_{25'} - \Gamma_1)$ energy differences.

^bReference 21.

^cS. Chatterjee and D. K. Chakraborti, J. Phys. F **1**, 638 (1971).

^dS. L. Altmann, A. R. Harford, and R. S. Blake, J. Phys. F **1**, 791 (1971).

where $E_d = k_d^2$ and

$$\langle \vec{k}_d | \Delta | \varphi_d \rangle = -4\pi Y_{2m}(\vec{k}_d) \Delta(k_d). \quad (29)$$

Of more direct interest, however, is the behavior of $\langle \vec{k} | \Delta | \varphi_d \rangle$ for $|\vec{k}| < k_F$, since the form factor and the total energy for the alkaline earths depend only on the hybridization within the Fermi sea. Figure 3 illustrates the effect of v^{loc} on $\Delta(k)$ for calcium. Note that for $k < k_F$, $|\Delta(k)|$ decreases as α_{sw} increases but becomes insensitive to v^{loc} for $\alpha_{sw} \geq 5$. Also note that the first maximum in $|\Delta(k)|$ tends to occur near $k = k_d$ for $\alpha_{sw} \geq 5$.

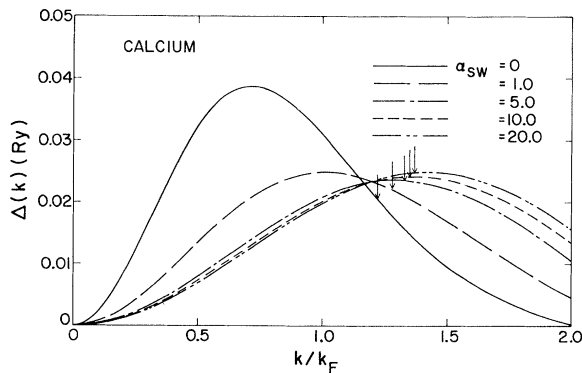


FIG. 3. Hybridization matrix element $\Delta(k) = -\langle \vec{k} | \Delta | \varphi_d \rangle / [4\pi Y_{2m}(k)]$ of calcium for five different values of the square-well depth. The arrows indicate the appropriate values of $k_d = E_d^{1/2}$.

V. APPLICATIONS

We now consider the question of how hybridization and d -state overlap affect the form factors and the total energy, and, hence, the electronic and atomic properties of the alkaline-earth metals. In order to do this systematically, we have defined five separate models for the hybridization and overlap. For future reference these models are summarized in Table III. Model *A* corresponds to the simple-metal limit in which $\langle \vec{r} | \varphi_d \rangle = 0$. Model *B* represents the opposite extreme in which we take $\langle \vec{r} | \varphi_d \rangle$ as the unlocalized ionic d state defined in Sec. II. In the remaining models, *C*, *D*, and *E*, the d state has been localized via $v^{loc}(r)$ with $\alpha_{sw} = 1.0, 5.0$, and 10.0 , respectively. In general, the quantities considered below converge more rapidly as a function α_{sw} than does either E_d or $\langle \vec{k} | \Delta | \varphi_d \rangle$. For this reason, we have not defined models for $\alpha_{sw} > 10.0$.

TABLE III. Summary of the five models defined in the text.

Model	Hybridization		Comments
	overlap	α_{sw}	
A	No	...	Simple-metal limit
B	Yes	0.0	Ionic d state
C	Yes	1.0	...
D	Yes	5.0	...
E	Yes	10.0	...

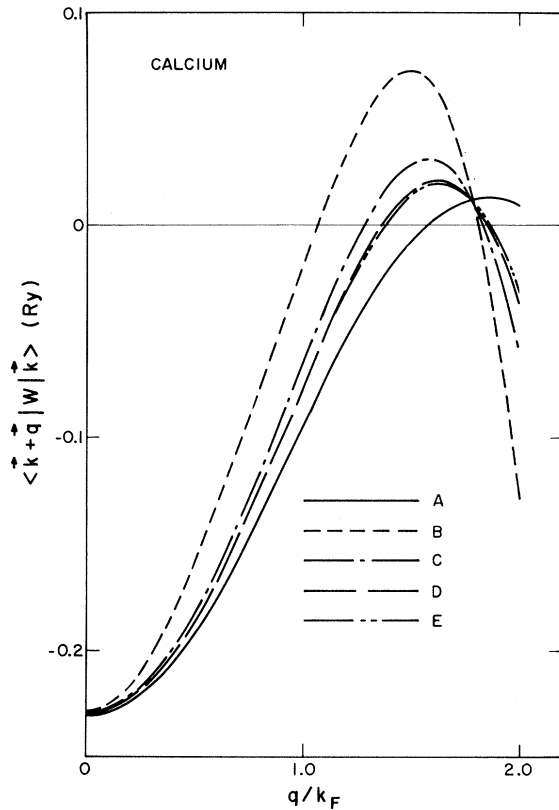


FIG. 4. Form factor of calcium for models A–E.

A. Form Factors and Electronic Properties

The form factor $\langle \vec{k} + \vec{q} | w | \vec{k} \rangle$ is one of the principal ingredients needed in the calculation of the electronic properties of a metal. Figure 4 shows the form factors we have calculated for calcium with models A–E. Note that in each case $\langle \vec{k} + \vec{q} | w | \vec{k} \rangle$ exhibits a maximum for $q < 2k_F$. The inclusion of hybridization increases the strength of this maximum and moves it toward $q = 0$ in such a way that $\langle \vec{k} + \vec{q} | w | \vec{k} \rangle$ takes on a relatively large negative value at $q = 2k_F$. The form factors for strontium and barium exhibit the same qualitative features. Figure 5 shows the form factors for all three metals calculated with model D, while Table IV gives the values of $\langle \vec{k} + \vec{q} | w | \vec{k} \rangle$ at $q = 2k_F$

TABLE IV. The form factor $\langle \vec{k} + \vec{q} | w | \vec{k} \rangle$ at $q = 2k_F$ for the alkaline-earth metals, in Ry.

Metal	HAA		Model				
	I ^a	II ^a	A	B	C	D	E
Ca	+0.007	-0.002	+0.010	-0.129	-0.060	-0.036	-0.032
Sr	...	-0.004	-0.002	-0.185	-0.067	-0.038	-0.035
Ba	-0.032	-0.032	-0.012	-0.509	-0.145	-0.073	-0.064

^aReference 16.

TABLE V. Resistivity of the liquid metal, in $\mu\Omega$ cm, calculated with various form factors and the Ashcroft–Lekner structure factor (Ref. 18).

Metal	Experiment ^a	HAA-I ^b	ZEC ^a	Model				
				A	B	C	D	E
Ca	33.0	15.5	16.4	11.9	190	40.5	17.5	15.2
Sr	84.8	...	7.2	7.2	592	71.5	24.5	20.8
Ba	306	15.4	12.2	8.6	5810	444	110	84.0

^aJ. B. Van Zytveld, J. E. Enderby, and E. W. Colings, J. Phys. F 2, 115 (1972). The theoretical values (ZEC) were computed at liquid densities by the Heine–Abarenkov model-potential method (Ref. 15).

^bForm factors from Ref. 16; resistivity values quoted from Ref. 18.

for each of the five models. For comparison corresponding values of the Heine–Abarenkov form factors¹⁵ calculated by Animalu¹⁶ are also listed in Table IV. Note that there is rough agreement between these latter values and our results for model A.

We have made a simple application of the form factors discussed above to the calculation of the resistivity of the liquid metal using the well-known Ziman formula.¹⁷ This calculation involves an

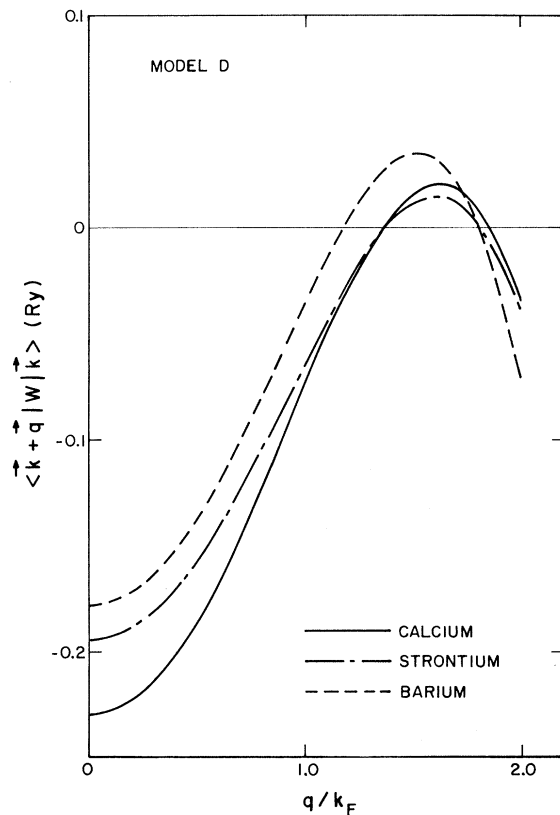


FIG. 5. Form factors of calcium, strontium, and barium for model D.

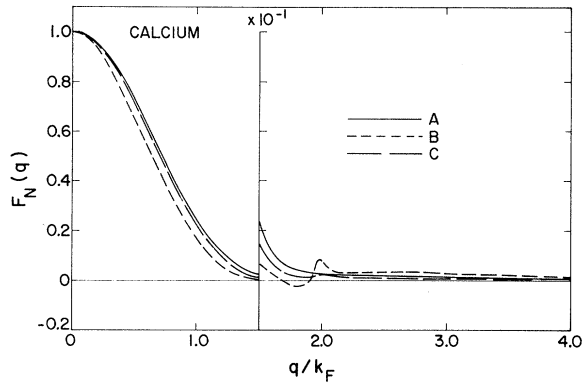


FIG. 6. Normalized energy-wave-number characteristic of calcium for models A-C.

integral of the intensity function (structure factor squared) times the form factor squared over the free-electron Fermi surface. Unfortunately, there is no experimental information on the structure factors of calcium, strontium, or barium. In lieu of such information, we have used the theoretical hard-sphere model¹⁸ for the structure factor with an assumed packing density of 0.45. The latter structure factor shows good agreement with experiment in the region of interest ($q \leq 2k_F$) for most simple metals,^{18,19} in particular potassium¹⁸ to the left of, and magnesium¹⁹ above, calcium in the Periodic Table.

The resistivity values we have calculated are listed in Table V together with the experimentally measured values and other theoretical results obtained with simple-metal form factors and the Ashcroft-Lekner structure factor.¹⁸ Because of the uncertainty in the structure factor (and also the fact that our calculations were performed at solid rather than liquid densities), little quantitative significance can be attached to the theoretical results. Nevertheless, several interesting qualitative features can be seen from Table V. Note first that the simple-metal form factors consistently lead to resistivity values much smaller than the experimental ones, especially for strontium and barium. The inclusion of hybridization clearly

TABLE VI. Binding energy for the alkaline-earth metals, in Ry. The values in parentheses are the experimental cohesive energies.

Metal	Experiment ^a	Model				
		A	B	C	D	E
Ca	-1.457 (0.134)	-1.361	-1.270	-1.347	-1.373	-1.378
Sr	-1.355 (0.124)	-1.206	-0.528	-1.093	-1.188	-1.200
Ba	-1.256 (0.137)	-0.888	+1.472	-0.679	-0.857	-0.878

^aThe experimental binding energy is equal in magnitude to the cohesive energy plus the first and second ionization energies of the free atom.

TABLE VII. Band-structure energy (top number) and the overlap energy (bottom number) for the alkaline-earth metals, in Ry. The values listed are for the fcc structure except where noted.

Metal	Model				
	A	B	C	D	E
Ca	-0.0159	-0.0198	-0.0134	-0.0146	-0.0157
	0.0	-0.0817	-0.0077	-0.0005	-0.0001
Sr	-0.0164	-0.0273	-0.0120	-0.0132	-0.0138
	0.0	-0.2569	-0.0116	-0.0005	-0.0000
Ba	-0.0226	-0.0065	-0.0311	-0.0266	-0.0271
	0.0	-0.8847	-0.0341	-0.0009	-0.0000
Ba (bcc)	-0.0222	+0.2232	-0.0124	-0.0216	-0.0233
	0.0	-0.8939	-0.0342	-0.0010	-0.0000

allows for substantially larger values of the resistivity, and for each metal theory and experiment can be made to agree with a value of α_{sw} between 0 and 5. Finally, note that in models B-E hybridization has ordered the resistivities such that calcium always has the smallest value and barium the largest in agreement with experiment.

B. Binding Energy

The binding energy per ion of the valence electrons in the metal is just E_{total} as defined by Eq. (18). We have evaluated E_{total} for the alkaline earths in their observed lattice structures (see

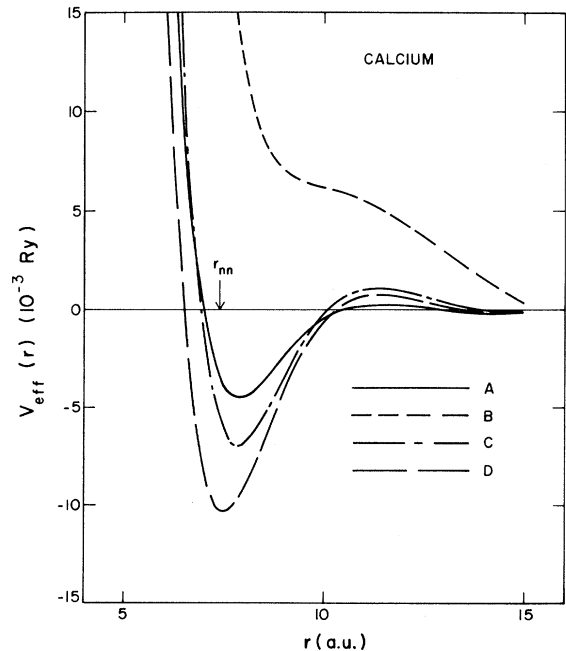


FIG. 7. Effective interaction potential of calcium for models A-D. The arrow indicates the nearest-neighbor distance r_{nn} .

Table VIII) for models $A-E$. These results together with the experimentally determined binding energies are listed in Table VI. Note that model B gives a rather poor result for strontium and an unreasonable result for barium. This is a consequence of the large values of $(E_d - E_F)^{-1}$ which accompany model B for these metals (see Table II). Also note that agreement with experiment improves for each metal as α_{sw} is increased. Last, it can be seen from Table VI that the difference in energy between E_{total} for model A and that for model E is much less than the cohesive energy in each case. This suggests that hybridization plays no important role in the cohesion of the alkaline-earth metals.

Equally as interesting are the values of the four components of E_{total} in our five models. The free-electron energy and the electrostatic energy have the largest magnitudes, and these quantities alone determine the first two significant figures in E_{total} , except in model B in which anomalously large values of the overlap energy occur. The electrostatic energy depends only on Z^* and the geometrical arrangement of the ions and is determined rather precisely. Our evaluation of E_{te} , on the other hand, is quite approximate due to the relatively crude formula we use for the exchange and correlation energy E_{xc} . The correct exchange and correlation energy probably lies somewhere between the uniform electron-gas value for an electron density Z/Ω_0 and that for an electron density Z^*/Ω_0 . This difference is comparable to the cohesive energy itself and is sufficient to explain the discrepancies between theory and experiment in E_{total} for calcium and strontium, although not for barium. Of course, the error in E_{te} is of no consequence in calculations which involve only the structure-dependent terms in the total energy, such as those considered below.

The variation of the structure-dependent band-structure energy and overlap energy with $|\varphi_d\rangle$ is illustrated in Table VII. The band-structure energy is only a function of the values of the energy-wave-number characteristic at reciprocal-lattice vectors. Figure 6 shows the normalized energy-wave-number characteristic

$$F_N(q) = -(q^2 \Omega_0 / 4\pi Z^*) F(q) \quad (30)$$

for calcium in models $A-C$. The curves for models D and E lie between those of models A and C and have been omitted from the figure for clarity. Note in particular that $F_N(q)$ in model B actually becomes negative near $q = 2k_F$. This behavior results from an overestimate of the hybridization contributions to $F(q)$ in model B and is even more pronounced in strontium and barium. In barium this anomaly leads to an unrealistically large energy difference between the fcc and bcc struc-

tures, as can be seen from Table VII.

The overlap energy has been evaluated by an approximate procedure analogous to that used for the noble metals.⁵ Specifically, to evaluate the matrix element $\langle \varphi_d | \Delta | \varphi_{d'} \rangle$, we have employed a modified form of δV in which the Coulomb potential arising from the neighboring ion in question is taken into account. The right-hand side of Eq. (25) was then fitted to a simple analytic form. Table VII shows just how rapidly the overlap energy thereby calculated decreases as $\langle \vec{r} | \varphi_d \rangle$ is localized. In particular, note that the overlap energy is unreasonably large for $\alpha_{sw} = 0.0$, especially for strontium and barium, while, on the other hand, it is essentially negligible for all three metals for $\alpha_{sw} \geq 5$.

C. Effective Interaction Potential

In passing we should point out here that the total energy can also be written in terms of a two-body effective interaction potential between ions, $v_{eff}(r)$:

$$E_{total} = E_0(\Omega_0) + \frac{1}{2} \sum_{i,j}' v_{eff}(|\vec{r}_i - \vec{r}_j|), \quad (31)$$

where E_0 depends only on the atomic volume Ω_0 and

$$v_{eff}(r) = \frac{2Z^*}{r} - \frac{4Z^*}{\pi} \int_0^\infty F_N(q) \frac{\sin qr}{qr} dq + v_{oi}(r). \quad (32)$$

The first term on the right-hand side of Eq. (32) is the direct Coulomb repulsion between ions of charge Z^*e , which arises from the electrostatic energy.

Figure 7 shows the effective interaction potentials we have calculated for calcium with models $A-D$. The curve for model E is almost the same as that for model D and is omitted for clarity. Note that, except for model B , there is a distinct minimum occurring just outside the nearest-neighbor distance r_{nn} in each case. The minimum deepens and moves toward r_{nn} as α_{sw} is increased. Also note the onset of the familiar Friedel oscillations at large r .

The above transformation to a real-space representation of the total energy, of course, offers no computational advantage in practice. The band-structure energy, for instance, converges much faster in reciprocal space than in real space. For this reason, we shall make no further use of $v_{eff}(r)$ in this paper.

D. Phonon Spectrum

Only a knowledge of the structure-dependent terms in E_{total} is needed to compute the phonon spectrum of a metal. The formulas for the eigenfrequencies $\omega(q)$ in terms of E_{es} , E_{bs} , and E_{oi} are well known and adequately discussed elsewhere.^{2,7,8} In brief, for a given structure and a given atomic volume, the only input information needed is the

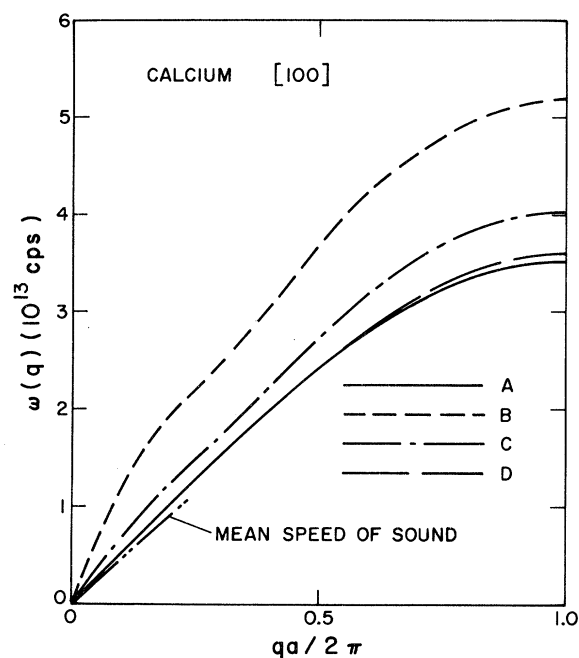


FIG. 8. Longitudinal-phonon frequencies of calcium in the [100] direction for models A–D. Also indicated is the experimental mean longitudinal speed of sound.

mass of the vibrating ion, the effective valence Z^* , the energy-wave-number characteristic $F(q)$, and the overlap potential $v_{o1}(r)$. From these quantities, we have calculated the fcc phonon frequencies of the alkaline-earth metals along the principal symmetry directions for all five models. Figure 8 shows the longitudinal modes of calcium in the [100] direction for models A–D. The dispersion curve for model E lies approximately between those of models A and D and has again been omitted for clarity. The contribution of the overlap energy to $\omega(q)$ in calcium is quite small (~ 1 – 3%) for $\alpha_{sw} = 0.0$ and is utterly negligible for $\alpha_{sw} \geq 1.0$. The hybridization contribution to $\omega(q)$ is relatively large, but clearly it is still very small for $\alpha_{sw} \geq 5.0$. No experimental phonon spectra have been measured for the alkaline-earths and our only contact with experiment here is through the mean longitudinal and transverse speeds of sound. The measured mean longitudinal speed of sound for calcium is indicated on Fig. 8 and clearly is most consistent with the dispersion curves for models A, D, and E.

The same over-all qualitative picture emerges for the other phonon modes of calcium as well as for the phonon spectra of strontium and barium. (In barium, however, the phonon frequencies generally turn out to be imaginary at small q with model B.) In Fig. 9 we have plotted the complete phonon spectra for calcium, strontium, and

barium calculated with model D.

Pseudopotential calculations of $\omega(q)$ for the alkaline earths had previously been done by Anilmalu²⁰ using the HAA-II and HAA-III form factors.¹⁶ His results generally show semiquantitative agreement with ours for models A, C, D, and E. His HAA-III phonon spectrum for strontium, in fact, shows fairly good quantitative agreement with our results. This latter finding has an interesting consequence, which we shall discuss below.

E. Phase Stability

As our final example, we shall briefly consider the subject of phase stability in the alkaline-earth

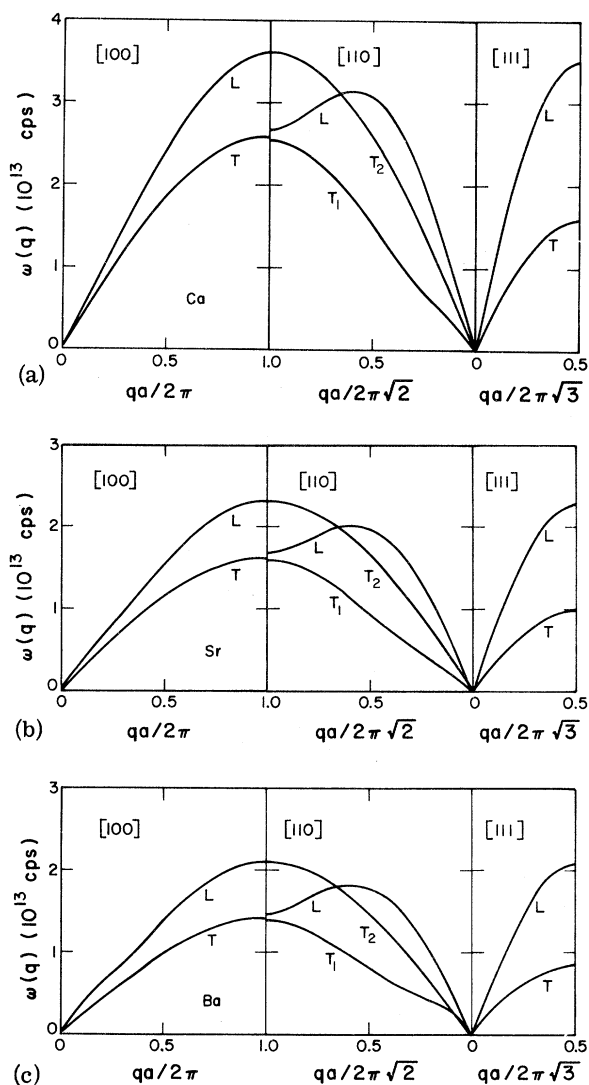


FIG. 9. fcc phonon frequencies of the alkaline-earths along principal symmetry directions for model D: (a) calcium, (b) strontium, and (c) barium.

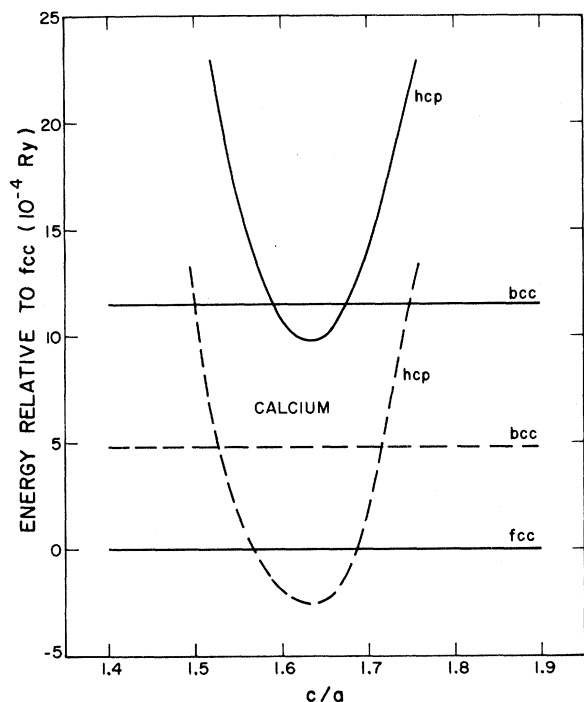


FIG. 10. Total energy of calcium as a function of lattice structure. The solid lines for the hcp and bcc structures refer to model D , while the dashed lines refer to model A .

metals. At zero temperature and pressure, one again only needs the structure-dependent terms in the total energy to determine the relative stability of two different crystal structures. (The difference in zero-point vibrational energies is usually negligible. This has been confirmed for the alkaline earths by Animalu.²⁰) The crystal structure which has the lowest total energy should be the one which is most stable.

We have computed the total energies of calcium, strontium, and barium in each of nine different crystal structures [fcc, bcc, and hcp at c/a axial ratios of 1.5, 1.6, 1.63 (ideal), 1.7, 1.8, 1.9, and 2.0] with models A - E . The predicted stable structures are listed in Table VIII together with the experimentally observed ones. Note that models B - E all give the correct fcc structure for calcium and for strontium, but that none of our models predict the observed bcc structure for barium. (For comparison the results obtained by Animalu²⁰ with the HAA-II and HAA-III form factors¹⁶ are also listed in Table VIII.) Figure 10 shows graphically the relative total energies of the various lattice structures of calcium for model A and for model D . Note that in both cases the hcp structure with the lowest total energy has the ideal c/a axial ratio. This is generally found to be the case. In Fig. 11 we have plotted for all

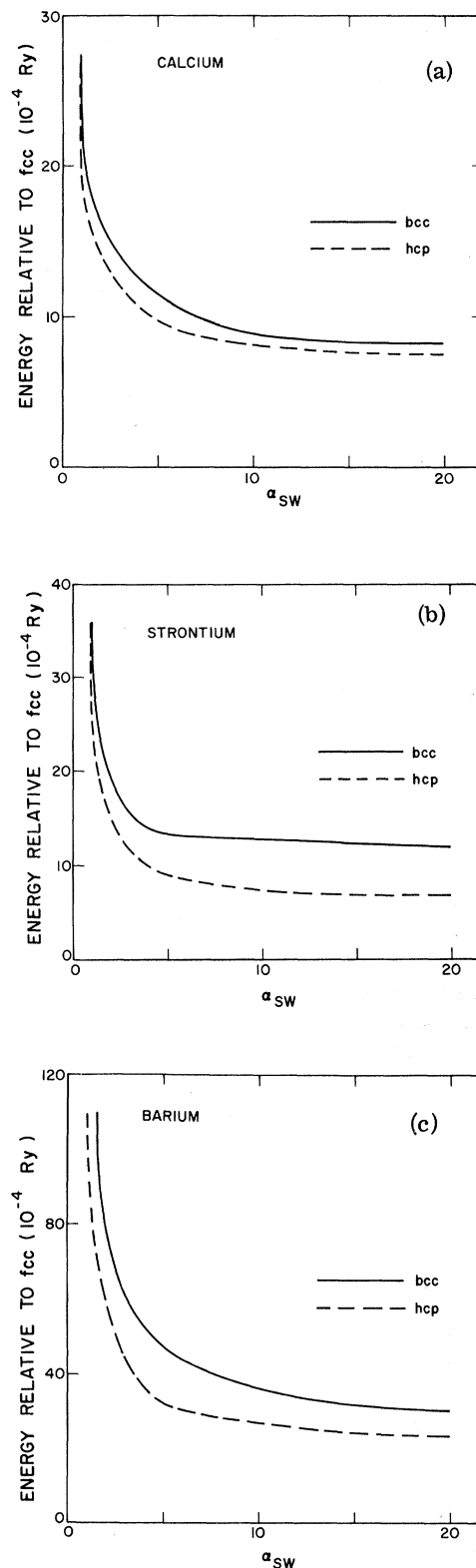


FIG. 11. Total energy of the bcc and the ideal hcp structures relative to that of the fcc structure as a function of square-well depth: (a) calcium, (b) strontium, and (c) barium.

TABLE VIII. Low-temperature stable phase for the alkaline-earth metals.

Metal	Observed	HAA-II ^a	HAA-III ^a	A	Model			
					B	C	D	E
Ca	fcc	bcc	bcc	hcp ^b	fcc	fcc	fcc	fcc
Sr	fcc	bcc	fcc	hcp ^b	fcc	fcc	fcc	fcc
Ba	bcc	bcc	bcc	fcc	hcp ^c	fcc	fcc	fcc

^aReference 20. See also Ref. 16. Only the energies of the fcc and bcc structures were compared in these calculations.

^b $c/a=1.63$.

^c $c/a=2.0$.

three metals the total energy of both the bcc and the ideal hcp structure relative to that of the fcc structure as a function of α_{sw} . For each metal the energy differences are unreasonably large for $\alpha_{sw}=0.0$ (model B), but decrease rapidly to acceptable limits as $\alpha_{sw} \rightarrow \infty$.

The phase-stability question is especially interesting in the alkaline-earth metals because of the temperature- and pressure-induced transitions which are observed in these metals. Animalu²⁰ has made a relatively extensive theoretical investigation of fcc-bcc phase transitions in these metals. His work, of course, was done in the spirit of the simple-metal pseudopotential theory. It is now quite interesting to attempt to reinterpret his findings in light of the generalized pseudopotential theory.

In brief, Animalu compared free energies of the bcc and the fcc phases of the alkaline earths as a function of temperature and pressure. He computed the relative free energy of the two phases as a sum of a zero-temperature electronic contribution (i. e., the contribution from the structure-independent terms in E_{total}) and a phonon contribution. It seems clear in retrospect that Animalu did poorly in estimating the former because the large effect of hybridization (as exemplified in Fig. 10) had, of course, been neglected. On the other hand, he did relatively well in estimating the phonon contribution, because of the rather small effect hybridization has on the phonon spectrum as was noted above. This seems to explain his qualitatively successful calculation of the temperature-pressure phase diagram for strontium. In particular, at zero pressure if Animalu's electronic contribution (1.9×10^{-4} Ry) is replaced with a more realistic value (e. g., the 13.4×10^{-4} Ry from model D), one would predict an fcc-to-bcc phase transition very near the observed transition temperature of 830 °K. More specifically, one obtains transition temperatures of approximately 1000, 950, and 900 °K for $\alpha_{sw}=5.0$, 10.0, and 20.0, respectively, as compared with the value of 150 °K found by Animalu.

Calcium exhibits a similar temperature-induced

fcc-to-bcc phase transition. Since, unlike Animalu, we can correctly predict a stable fcc structure at zero temperature and pressure in this metal, we would expect this transition to also be explainable in terms of our theory. Barium, on the other hand, is already bcc at zero temperature and pressure. Our incorrect predictions of a stable fcc structure for barium may be a consequence of our neglect of the f resonance (in addition to the d resonance) not far above the Fermi level in this metal. The band-structure calculations of Kmetko,²¹ for example, show an unoccupied f band only about 0.25 Ry above the unoccupied d band.

VI. CONCLUSIONS

From a purely practical standpoint, it is clear that the localized d states we have constructed make better basis states for the alkaline-earth metals than do the pure ionic d states. Although our method does not single out a "best" choice of $|\varphi_d\rangle$, our calculations suggest that there is probably a range of d states with which meaningful calculations can be done. Clearly, we have seen that the physical properties, especially the atomic properties, are not highly sensitive to the depth of the square well for $\alpha_{sw} \geq 5$. The quantitative difference between the results for two similar calculations, one done with $\alpha_{sw}=5.0$ and the other with $\alpha_{sw}=20.0$, is actually less than or equal to the absolute uncertainty in either calculation. This fact can be appreciated by noting the difference in E_d between methods 1 and 2 in Fig. 2 and is consistent with the observation that for $\alpha_{sw}=5.0$ the spatial extent of the d state for each of the alkaline earths is roughly the same as that of the s and p core states of the same principal quantum number (e. g., the $3s$ and $3p$ states in calcium). In this sense, we judge the results obtained in calculations with $\alpha_{sw} > 5.0$ to be equivalent to those obtained with $\alpha_{sw}=5.0$. For future reference we have tabulated the form factors and normalized energy-wave-number characteristics calculated with $\alpha_{sw}=5.0$ (model D) in Table IX.

From a theoretical point of view, the introduction of a seemingly arbitrary potential v^{loc} is the price one must pay to construct rapidly convergent expansions in the hybridization potential Δ . Conceivably, one could use some optimization criterion to pick v^{loc} uniquely, such as requiring that it lead to the correct d phase shift of the total potential. There is, of course, no fundamental significance to the square-well form for v^{loc} that we have used here. Our success with the square well seems to be attributable to two things. First, by localizing $\langle \vec{r} | \varphi_d \rangle$ we have effectively allowed for a more accurate calculation of both E_d and $\langle \vec{k} | \Delta | \varphi_d \rangle$ because Eq. (26) for $\delta V(r)$ is clearly a better ap-

proximation for small r than for large r . Second, there is an obvious tendency for variations in $\langle \vec{r} | \varphi_d \rangle$ to be compensated for by changes in Δ , so that the details of v^{loc} become of secondary im-

portance. We would expect, therefore, that other forms of v^{loc} would work equally as well.

The use of highly localized d states for pseudopotential calculations on other d -band metals holds

TABLE IX. Form factors and normalized energy-wave-number characteristics for the alkaline-earth metals from model D , in a.u. (For $q \leq 2k_F$ in $\langle \vec{k} + \vec{q} | w | \vec{k} \rangle$, $|\vec{k}| = |\vec{k} + \vec{q}| = k_F$. For $q > 2k_F$, $|\vec{k}| = k_F$ and \vec{k} and \vec{q} are antiparallel.)

q/k_F	Ca ($Z^* = 2.3997$)		Sr ($Z^* = 2.5041$)		Ba ($Z^* = 2.7359$)	
	$\langle \vec{k} + \vec{q} w \vec{k} \rangle$	$F_N(q)$	$\langle \vec{k} + \vec{q} w \vec{k} \rangle$	$F_N(q)$	$\langle \vec{k} + \vec{q} w \vec{k} \rangle$	$F_N(q)$
0.00	-0.2300	1.000 00	-0.1944	1.000 00	-0.1778	1.000 00
0.10	-0.2282	0.988 29	-0.1929	0.987 92	-0.1761	0.987 22
0.20	-0.2234	0.953 77	-0.1888	0.952 35	-0.1719	0.949 68
0.30	-0.2140	0.898 26	-0.1810	0.895 22	-0.1630	0.889 55
0.40	-0.2022	0.824 13	-0.1711	0.819 28	-0.1523	0.809 63
0.50	-0.1864	0.735 71	-0.1579	0.728 94	-0.1375	0.715 01
0.60	-0.1684	0.636 73	-0.1427	0.628 49	-0.1211	0.610 07
0.70	-0.1475	0.533 13	-0.1252	0.523 81	-0.1017	0.501 64
0.80	-0.1250	0.429 45	-0.1062	0.419 92	-0.0811	0.394 88
0.90	-0.1011	0.331 40	-0.0861	0.322 26	-0.0593	0.296 07
1.00	-0.0768	0.243 28	-0.0656	0.235 32	-0.0373	0.209 81
1.10	-0.0531	0.168 32	-0.0457	0.161 92	-0.0165	0.139 21
1.20	-0.0308	0.109 11	-0.0270	0.104 54	0.0028	0.086 31
1.30	-0.0115	0.065 20	-0.0109	0.062 30	0.0183	0.049 86
1.40	0.0044	0.036 15	0.0023	0.034 56	0.0297	0.027 79
1.50	0.0153	0.018 68	0.0109	0.017 80	0.0348	0.016 05
1.60	0.0206	0.009 65	0.0148	0.009 04	0.0331	0.009 94
1.70	0.0189	0.005 47	0.0123	0.004 70	0.0225	0.006 38
1.80	0.0096	0.003 38	0.0033	0.002 62	0.0023	0.003 87
1.90	-0.0083	0.002 39	-0.0133	0.001 83	-0.0291	0.003 59
2.00	-0.0358	0.002 67	-0.0382	0.002 32	-0.0729	0.006 30
2.10	-0.0389	0.001 89	-0.0406	0.001 38	-0.0795	0.003 56
2.20	-0.0410	0.001 51	-0.0420	0.001 05	-0.0835	0.002 81
2.30	-0.0418	0.001 18	-0.0420	0.000 82	-0.0846	0.002 37
2.40	-0.0412	0.000 92	-0.0404	0.000 68	-0.0828	0.002 12
2.50	-0.0390	0.000 72	-0.0374	0.000 61	-0.0782	0.002 01
2.60	-0.0353	0.000 60	-0.0329	0.000 61	-0.0709	0.001 98
2.70	-0.0304	0.000 54	-0.0272	0.000 67	-0.0613	0.002 01
2.80	-0.0244	0.000 54	-0.0205	0.000 75	-0.0499	0.002 07
2.90	-0.0177	0.000 58	-0.0132	0.000 86	-0.0373	0.002 13
3.00	-0.0105	0.000 64	-0.0055	0.000 97	-0.0239	0.002 18
3.10	-0.0034	0.000 71	0.0021	0.001 06	-0.0104	0.002 21
3.20	0.0036	0.000 78	0.0094	0.001 13	0.0028	0.002 21
3.30	0.0100	0.000 83	0.0161	0.001 17	0.0151	0.002 18
3.40	0.0156	0.000 86	0.0219	0.001 18	0.0262	0.002 11
3.50	0.0202	0.000 87	0.0267	0.001 15	0.0357	0.002 00
3.60	0.0238	0.000 86	0.0304	0.001 09	0.0434	0.001 86
3.70	0.0262	0.000 83	0.0328	0.001 02	0.0492	0.001 69
3.80	0.0274	0.000 79	0.0340	0.000 93	0.0530	0.001 51
3.90	0.0275	0.000 74	0.0340	0.000 83	0.0548	0.001 33
4.00	0.0265	0.000 68	0.0329	0.000 73	0.0547	0.001 14
4.10	0.0247	0.000 63	0.0308	0.000 63	0.0529	0.000 97
4.20	0.0221	0.000 58	0.0280	0.000 55	0.0496	0.000 82
4.30	0.0189	0.000 53	0.0245	0.000 47	0.0451	0.000 69
4.40	0.0153	0.000 50	0.0205	0.000 41	0.0397	0.000 58
4.50	0.0115	0.000 46	0.0164	0.000 36	0.0336	0.000 49
4.60	0.0077	0.000 44	0.0122	0.000 33	0.0271	0.000 43
4.70	0.0041	0.000 42	0.0081	0.000 30	0.0206	0.000 39
4.80	0.0007	0.000 39	0.0043	0.000 27	0.0143	0.000 35
4.90	-0.0022	0.000 38	0.0009	0.000 25	0.0085	0.000 33
5.00	-0.0046	0.000 36	-0.0020	0.000 24	0.0033	0.000 31

considerable promise. Such a representation is certainly desirable from the standpoints of simplicity and calculational accuracy. Moreover, the generalization of the methods of Sec. II to other d -band metals is quite straightforward. The major qualitative difference we foresee is that the core states will be affected by changes in the d states in

cases where the latter are partially or fully occupied.

ACKNOWLEDGMENT

The author wishes to thank Dr. John H. Wood for supplying his version of the Herman-Skillman computer program and for helpful discussions and technical advice on the free-ion calculations.

*Work performed under the auspices of the U. S. Atomic Energy Commission.

¹W. A. Harrison, Phys. Rev. **181**, 1036 (1969).

²J. A. Moriarty, Ph.D. thesis (Stanford University, 1970) (unpublished).

³J. A. Moriarty, Phys. Rev. B **5**, 2066 (1972).

⁴J. A. Moriarty, Phys. Rev. B **1**, 1363 (1970).

⁵J. A. Moriarty, Phys. Rev. B **6**, 1239 (1972).

⁶See, for example, E. Brown and J. A. Krumhansl, Phys. Rev. **109**, 30 (1958) [applied to copper by F. A. Butler, F. K. Bloom, Jr., and E. Brown, *ibid.* **180**, 744 (1969)]; R. A. Deegan and W. D. Twose, *ibid.* **164**, 993 (1967).

⁷W. A. Harrison, *Pseudopotentials in the Theory of Metals* (Benjamin, New York, 1966).

⁸V. Heine and D. Weaire, in *Solid State Physics*, edited by F. Seitz, D. Turnbull, and H. Ehrenreich (Academic, New York, 1970), Vol. 24.

⁹We use the atomic units $\hbar = 2m = \frac{1}{2}e^2 = 1$ throughout. In these units energies are in rydbergs and lengths are in Bohr radii.

¹⁰F. Herman and S. Skillman, *Atomic Structure Calculations* (Prentice Hall, Englewood Cliffs, N. J., 1963).

¹¹B. J. Austin, V. Heine, and L. J. Sham, Phys. Rev.

127, 276 (1962).

¹²M. H. Cohen and V. Heine, Phys. Rev. **122**, 1821 (1961).

¹³K. S. Singwi, M. P. Tosi, R. H. Land, and A. Sjölander, Phys. Rev. B **1**, 1044 (1970).

¹⁴See, for example, C. Kittel, *Quantum Theory of Solids* (Wiley, New York, 1963), p. 114.

¹⁵V. Heine and I. Abarenkov, Phil. Mag. **9**, 451 (1964).

¹⁶Several sets of form factors for the alkaline-earth metals have been calculated by Animalu. The original set (HAA-I), which included only calcium and barium, was reported by A. O. E. Animalu and V. Heine [Phil. Mag. **12**, 1249 (1965)] and is tabulated in Ref. 7. A second set (HAA-II) is given by A. O. E. Animalu [Proc. Roy. Soc. (London) **A294**, 376 (1966)]. Yet a third set (HAA-III) was used in Ref. 20.

¹⁷J. M. Ziman, Phil. Mag. **6**, 1013 (1961).

¹⁸N. W. Ashcroft and J. Lekner, Phys. Rev. **145**, 83 (1966).

¹⁹J. B. Van Zytveld (private communication).

²⁰A. O. E. Animalu, Phys. Rev. **161**, 445 (1967).

²¹E. A. Kmetko, *Electronic Density of States*, Natl. Bur. Std. (U. S. GPO, Washington, D. C., 1971).

Magnetoacoustic Evidence for the Existence of the L -Centered Pocket of Fermi Surface in Palladium*

C. R. Brown, J. P. Kalejs,† F. D. Manchester, and J. M. Perz
Department of Physics, University of Toronto, Toronto 5, Canada

(Received 22 June 1972)

Quantum oscillations in ultrasonic attenuation have been observed in Pd. We report a new frequency which is attributed to small hole pockets at the L symmetry points. Such pockets were predicted by theory but have not been seen in de Haas-van Alphen experiments. Measurements have been made of the angular variation of the extremal area of these pockets and of their cyclotron effective masses in the (100) plane.

I. INTRODUCTION

Relativistic-augmented-plane-wave (RAPW) band calculations for palladium by both Mueller *et al.*¹ and Andersen² have predicted small pockets of holes around the symmetry points L , but oscillations corresponding to such carriers were not observed in the detailed de Haas-van Alphen (dHvA) studies of Windmiller *et al.*³ We report here the frequencies of magnetoacoustic quantum oscilla-

tions in Pd, which we relate to the hole pockets at L . Our measurements yield cyclotron masses $m_c^* \approx 1.1m_0$, consistent with the theoretical predictions^{1,2} of low velocities for these holes. The low effective masses usually associated with small pockets normally assure adequate amplitudes for the various oscillatory effects; the absence of dHvA signals from the holes at L in Pd is probably a consequence of the unusually high m_c^* . Quantum oscillations in ultrasonic attenuation